Suspension-Line Wave Motion during the Lines-First Parachute Unfurling Process

LAMONT R. POOLE*
NASA Langley Research Center, Hampton, Va.
AND
JOHN L. WHITESIDES†
Joint Institute for Acoustics and Flight Sciences, Hampton, Va.

A new mathematical approach to modeling the lines-first parachute unfurling process is presented. The unfurling process is treated as two distinct phases: a suspension-line unfurling phase, during which a massless-spring model of the suspension-line elasticity may be employed; and a canopy unfurling phase, during which a formulation considering suspension-line wave mechanics is employed. Histories of unfurled length and tension at the vehicle obtained using the model are compared with flight test data, and generally good agreement is observed.

Nomenclature

A = reference area, m^2
C = damping coefficient of a single suspension line, N-sec
C_D = drag coefficient
F_{re} = unfurling resistance force, N
g = acceleration due to gravity, m/sec^2
h = altitude, m
K_{sec}' = specific secant modulus of a single suspension line, N
l = general spatial coordinate along unstressed suspension lines, measured from vehicle attachment point, m
l_B = unfurled length (or, equivalently, spatial coordinate of parachute mass element exiting mouth of deployment bag), m
L_p = total unstressed length of extended parachute, m
L_{sl} = unstressed length of suspension lines, m
m = mass, kg
m' = linear mass density of general parachute element exiting mouth of deployment bag, kg/m
m_{sl}' = linear mass density of a single suspension line, kg/m
n_{sl} = number of suspension lines
q = freestream dynamic pressure, N/m^2
t = time, sec
t_{mf} = time from mortar fire, sec
T = tension, N
u = unfurling rate or velocity at which parachute exits mouth of deployment bag, m/sec
v = velocity, m/sec
x = deployed distance of bag, measured rearward from base of vehicle, m
γ = flight-path angle, measured with respect to local horizontal, deg
δ = displacement of any cross section of suspension lines from its unstressed position, m
η = wake parameter

Subscripts

b = deployment bag
B = deployment bag mouth
e = deployment bag plus its contents
sl = suspension line
v = vehicle
V = suspension-line attachment point at vehicle
$\cdot$ = time derivative

Received June 4, 1973; revision received August 27, 1973. This paper is based in part on a thesis submitted to The George Washington University in partial fulfillment of the requirements for the M.S. degree.

Index categories: Entry Deceleration Systems and Flight Mechanics (e.g., Parachutes); Structural Dynamic Analysis.

* Aerospace Engineer, Space Applications and Technology Division.

† Assistant Research Professor, School of Engineering and Applied Science, The George Washington University. Member AIAA.

Introduction

THE successful operation of a parachute system depends not only on a proper inflation phase, during which large aerodynamic drag forces are generated by the inflating parachute, but also on a proper unfurling phase, during which the parachute is extended from a packed configuration to a stage at which the inflation phase can begin in a satisfactory manner. A lines-first-type unfurling sequence is the type chosen for most spacecraft applications. In a general lines-first unfurling process, the parachute suspension system and canopy are folded and packed into a deployment bag which is stowed in the spacecraft until desired trajectory conditions are reached. The bag is then deployed rearward from the vehicle, either by some forced-ejection device such as a mortar or by a small drogue or pilot parachute. As the bag travels rearward, the packed suspension system and, then, canopy are unfurled from the bag.

A primary need for simulating the unfurling process is to determine the motion of the deployment bag relative to the towing vehicle. Knowledge of sequence of events and unfurling times, the rates at which parachute material is unfurled from the deployment bag, and the levels of tension generated in the suspension system during the process of unfurling are important from mission analysis and deployment system design standpoints.

A strong effort in the past few years, stimulated by the selection of a parachute system as the primary means of deceleration for the Viking 75 mission to Mars, has led to significant advances in analytical modeling of unfurling and inflation dynamics. A synopsis of recent analytical developments is presented in Ref. 1; descriptions of those analytical models which apply specifically to the lines-first unfurling process are presented in Refs. 2–4. One over-all conclusion arising from the analytical effort was that all unfurling motions and the nearly steady loads characteristic of suspension-line unfurling could be simulated well using elementary models of the suspension-line elasticity, such as an inextensible or a massless-spring-type model. The analytical effort also demonstrated the promise of continuum-type treatment of the suspension lines in the simulation of the high-frequency loads characteristic of canopy unfurling.

This paper presents the basic concepts of a new mathematical model which employs the equations developed in Ref. 3 for governing the two-body planar motion of the lines-first forced-ejection unfurling process in conjunction with the one-dimensional nonlinear partial differential equation governing suspension-line wave motion. Boundary conditions on the wave motion are developed such that the formulation can be reduced to one of the massless-spring class during the phase of suspension-line unfurling. Numerical techniques are discussed which have

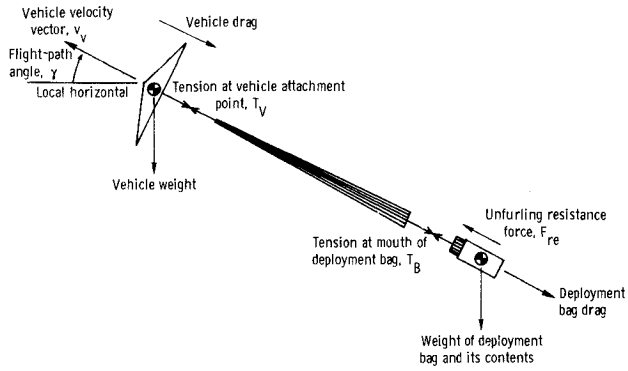

Fig. 1 Forces affecting motions of vehicle and deployment bag.

been developed for obtaining a solution to both the reduced set of equations in effect during the suspension-line unfurling phase and to the complete set of equations in effect during the canopy unfurling phase. The present model is used to calculate unfurling loads and motions of two disk-gap-band parachute deployment flight tests, and generally good agreement between calculated results and flight-test data is observed.

Analysis

In the analysis to follow, equations are presented which govern the motion of a towing vehicle and the motion of the deployment bag relative to the vehicle during the lines-first unfurling process. An expression is given relating the tension developed at the mouth of the deployment bag to the rate at which the unfurling parachute exits the mouth of the bag (the unfurling rate). Mathematical models by which the suspension-line elastic response can be approximated are discussed. The equation and general boundary conditions governing the motion for a continuum model of the suspension lines are developed. Specific boundary conditions are developed by which the unfurling process can be treated as two phases: a suspension-line unfurling phase, during which a mathematical model of the massless-spring type can be applied; and a canopy unfurling phase, during which a continuum-type model of the suspension-line response must be applied. A general discussion of numerical techniques which have been employed in the solution of equations governing both phases is included.

For the purposes of this analysis, the vehicle and the deployment bag and its instantaneous contents are considered to be mass particles. The surface of the planet is considered to be flat, and surface-relative accelerations are considered to be inertial. The towing vehicle is assumed to be nonlifting, and its motion is restricted to a vertical plane. The motion of the deployment bag relative to the vehicle and the orientation of the tension vector in the parachute suspension lines are assumed to be parallel to the vehicle relative wind.

Equations of Motion

The forces affecting the motion of the vehicle and deployment bag are shown in Fig. 1. From consideration of these forces, the equations governing the planar motion of the two bodies were developed in Ref. 3 and are summarized as follows:

Longitudinal acceleration of the vehicle

$$\dot{v}_v \doteq -\left[\frac{(C_D A)_v q_\infty + T_V}{m_v} + g\sin\gamma\right] \tag{1}$$

Longitudinal inertial acceleration of the deployment bag

$$\dot{v}_b = -\left[\frac{\eta(C_D A)_b q_\infty - F_{re}}{m_e} + g\sin\gamma\right] \tag{2}$$

Rate of change of altitude

$$\dot{h} = v_v \sin\gamma \tag{3}$$

Rate of change of flight-path angle

$$\dot{\gamma} = -g\cos\gamma/v_v \tag{4}$$

Velocity of the deployment bag relative to the vehicle (positive rearward)

$$\dot{x}_b = v_v - v_b \tag{5}$$

An additional expression was developed in Ref. 4 which defines the tension developed in the unfurling parachute at the mouth of the deployment bag as a function of the linear mass density of the parachute element exiting the bag, the unfurling rate, and the unfurling resistance force. This expression is

$$T_B = m'u^2 + F_{re} \tag{6}$$

The unfurling rate is, by definition, the rate of change of the spatial coordinate of the mouth of the deployment bag, or

$$u = \dot{l}_B \tag{7}$$

The linear mass density is a function of the unfurled length, and its distribution is a characteristic of the specific parachute design. The linear-mass-density profile for a typical disk-gap-band (DGB) parachute is shown in Fig. 2. The spikes in the distribution denote areas in the DGB canopy where several layers of cloth and tape are overlapped for reinforcement purposes.

The set of governing equations is indeterminate in that two parameters, namely, the unfurling rate u and the tension at the vehicle attachment point T_V, remain to be explicitly defined. In order to make the set of equations determinate, a mathematical model of the parachute elasticity must be employed. Since the parachute canopy is thought to undergo very little, if any, deformation during the unfurling process, it can be considered to be inextensible. The procedure can be idealized further by assuming that the suspension system consists of suspension lines only, with each suspension line having negligible aerodynamic drag and uniform mass and elastic properties. Thus, the procedure has been reduced to one of formulating a mathematical model of the elasticity of a single suspension line.

Candidate Mathematical Models of Suspension-Line Elasticity

1) The most elementary model of suspension-line elasticity is one that assumes the suspension lines to be inextensible. Such a model was employed in the analysis presented in Ref. 2. The choice of an inextensible-lines model defines the unfurling rate u and the tension at the vehicle T_V as follows:

$$u = \dot{x}_b$$

$$T_V = T_B + \int_0^{l_B} m'(\dot{v}_v + g\sin\gamma)\,dl$$

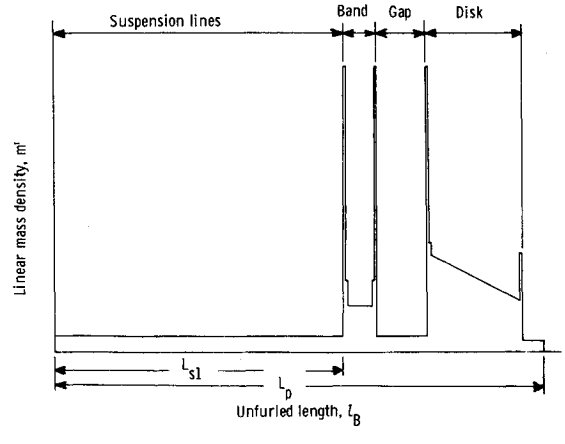

Fig. 2 Typical linear-mass-density distribution for disk-gap-band parachute.

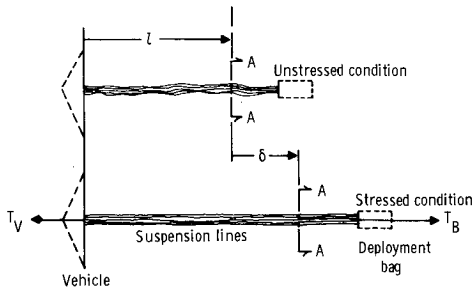

Fig. 3 Coordinates defining suspension-line geometry.

The integral in the previous equation denotes the force due to acceleration of the unfurled portion of the parachute. In using the inextensible model to simulate flight-test unfurling sequences, it was found that all unfurling motions and tension loads occurring during suspension-line unfurling could be simulated well. However, the very high frequency loads occurring during canopy unfurling which are caused by rapid fluctuations in the linear-mass-density of the material being unfurled (as depicted in Fig. 2) could not be simulated well.

2) Another elementary model of suspension-line elasticity is the massless-spring-type model, which was used in the analysis presented in Ref. 3. Choice of a massless-spring model defines the unfurling rate and the tension at the vehicle as follows:

$$u = u(\dot{x}_b, \varepsilon)$$
$$T_V = T_B$$

where ε is a uniform strain (i.e., is constant along the length of the suspension lines). In using the massless-spring model to simulate flight-test unfurling sequences, it was found that, again, all unfurling motions and the tension loads occurring during suspension-line unfurling could be simulated well, while the high-frequency tension loads occurring during canopy unfurling could not be simulated with appreciable accuracy.

3) One conclusion stated in Ref. 3 was that a mathematical model considering suspension-line wave mechanics would be needed in order to simulate the unfurling process more precisely. One benefit of such a model is that the unfurling rate and the tension at the vehicle can be calculated from boundary conditions on the suspension-line wave motion. The promise of such continuum-type modeling had been demonstrated by the results presented in Ref. 4. In that paper, an elementary treatment of the suspension-line wave mechanics was employed in the development of a closed-form technique for calculating the snatch force which is generated just as the canopy begins to unfurl from the deployment bag.

In a continuum sense, the elastic state of an arbitrary cross-section of the suspension lines can be represented by use of the coordinates and variables shown in Fig. 3. The basic equation governing the longitudinal motion of this arbitrary suspension-line element was developed in Ref. 3, and can be written as

$$\frac{\partial^2 \delta}{\partial t^2} - \frac{1}{n_{sl} m_{sl}'} \frac{\partial T}{\partial l} = -\left[\frac{(C_D A)_v q_\infty + T_V}{m_v}\right] \tag{8}$$

The tension at the arbitrary cross-section can be represented by a constitutive equation involving the displacement δ and its derivatives. The relationship employed in the present analysis represents the tension as the sum of static and dynamic components, and can be written as

$$T = n_{sl}[K_{sec}' \partial\delta/\partial l + C(\partial/\partial t)(\partial\delta/\partial l)] \tag{9}$$

where the specific secant modulus K_{sec}' and thus the wave propagation velocity, is a function of the strain $\partial\delta/\partial l$, and the damping coefficient C is a constant.

The suspension lines are assumed to be attached to the vehicle in such a manner that no deflection occurs at that point in the lines. Mathematically, this boundary condition can be stated as

$$\delta|_{l=0} = 0 \tag{10}$$

The tension in the suspension lines is subject to the boundary condition at the mouth of the deployment bag which is given in Eq. (6), or

$$T|_{l=l_B} = m'u^2 + F_{re}$$

An additional boundary condition which assures compatibility between the relative motion of the deployment bag and the motion of the parachute element exiting the mouth of the bag can be written as

$$D\delta/Dt|_{l=l_B} = \dot{x}_b - u \tag{11}$$

Two-Phase Model of Suspension-Line Elasticity

Suspension-Line Phase

The unfurling motions and nearly steady tension loads occurring during suspension-line unfurling can be simulated well, as stated previously, by using a massless-spring-type model of the suspension-line elasticity. The use of such a model in the present analysis concerning that phase would be of special benefit in that it would eliminate the necessity of solving the basic partial differential equation governing the suspension-line wave motion. An immediate result of assuming a massless-spring-type model is the definition of the tension at the vehicle, or as stated previously

$$T_V = T_B \tag{12}$$

Since the boundary at the mouth of the bag is moving during the suspension-line phase, the total derivative in Eq. (11) must be expanded into local and convective terms, or

$$\left.\frac{D\delta}{Dt}\right|_{l=l_B} = \left.\frac{\partial\delta}{\partial t}\right|_{l=l_B} + u\left.\frac{\partial\delta}{\partial l}\right|_{l=l_B} = \dot{x}_b - u \tag{13}$$

where u is again, equivalent to l_B. Since the loads are nearly steady, the assumption can be made that both the deflection rate $\partial\delta/\partial t$ and the strain rate $(\partial/\partial t)(\partial\delta/\partial l)$ at this boundary are nearly zero. Then the strain at the boundary can be found as a function of the tension at the bag mouth T_B by Eq. (9). Thus the boundary condition at the bag mouth has been reduced to the following expression:

$$uT_B/n_{sl} K_{sec}' = \dot{x}_b - u \tag{14}$$

T_B can be replaced in Eq. (14) by its definition as given in Eq. (6); the result is a cubic equation defining the equilibrium unfurling rate during the suspension-line phase.

$$u^3 + \frac{K_{sec}'}{m_{sl}'}\left(1 + \frac{F_{re}}{n_{sl} K_{sec}'}\right)u - \frac{K_{sec}'}{m_{sl}'}\dot{x}_b = 0 \tag{15}$$

Thus the governing equations for the suspension-line unfurling phase consist of ordinary differential equations and algebraic equations only. Since the ordinary differential equations of interest are very smooth in nature, numerical solutions can be obtained by a simple procedure such as the single-step forward-difference integration technique suggested by Euler.[5]

Canopy Phase

Proper treatment of the canopy unfurling phase must include simultaneous solutions of the ordinary differential equations governing vehicle and deployment-bag motion and the partial differential equation governing suspension-line wave motion. Since, the canopy is assumed to be inextensible, the rearward boundary for the wave motion is the juncture of the suspension lines and canopy, which is stationary in the spatial coordinate frame during the canopy unfurling phase. Thus the boundary condition expressed by Eq. (11) can be simplified to the following equation:

$$\partial\delta/\partial t|_{l=l_{sl}} = \dot{x}_b - u \tag{16}$$

By assuming that the tension is constant along the length of the unfurled portion of the canopy (acceleration of that portion of the canopy is neglected), the tension at the juncture equals the tension generated at the mouth of the deployment bag, which is expressed by Eq. (6).

The ordinary differential equations in effect during this phase

can again be integrated using Euler's technique. The basic equation governing suspension-line wave motion can be solved by employing standard explicit finite-difference formulations to approximate the partial derivatives $\partial^2\delta/\partial t^2$ and $\partial T/\partial l$. The solution to the wave equation at the juncture of the suspension lines and canopy requires compatible values for the unfurling rate and the tension gradient at the juncture, which must be obtained by an iterative procedure involving the coupled boundary conditions [Eqs. (6 and 16)] and the constitutive equation [Eq. (9)].

The tension at the vehicle T_V can be found by applying the wave equation [Eq. (8)] at the vehicle boundary, with $\partial^2\delta/\partial t^2 = 0$, in conjunction with a linearized Taylor's series expansion of the tension with respect to the spatial coordinate.

The numerical techniques discussed in this section are derived and presented in detail in Ref. 5. It was stated in that reference that a stable solution can be assured if the selection of a finite-difference grid pattern is made such that the ratio of the spatial grid unit to the temporal grid unit is greater than or equal to the maximum wave propagation velocity [the maximum value of $(K_{sec}'/m_{sl}')^{1/2}$]. Essentially identical solutions were obtained using several stable grid unit ratios.

Results and Discussion

In order to evaluate the accuracy of the two-phase method in the simulation of the unfurling process, the techniques presented in this paper were used to calculate unfurling loads and motions for two flight tests of disk-gap-band parachutes: the second balloon-launched flight test of the NASA Planetary Entry Parachute Program, B/L-2 (Ref. 6); and the flight test of vehicle AV-4 of the NASA Balloon-Launched Decelerator Test Program.[7] Descriptions of the input data used in the computer simulations are listed in Ref. 5.

Indicative of the accuracy of the present model in the simulation of unfurling motions are the computed histories of unfurled length for the two flight tests shown in Fig. 4. The computed histories are seen to agree very well with flight-test data points

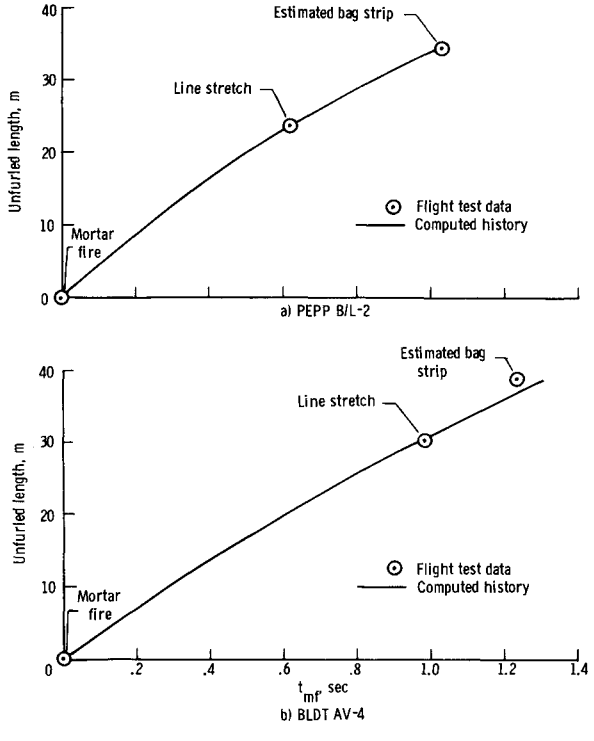

Fig. 4 Comparison of computed histories of unfurled length with flight-test data.

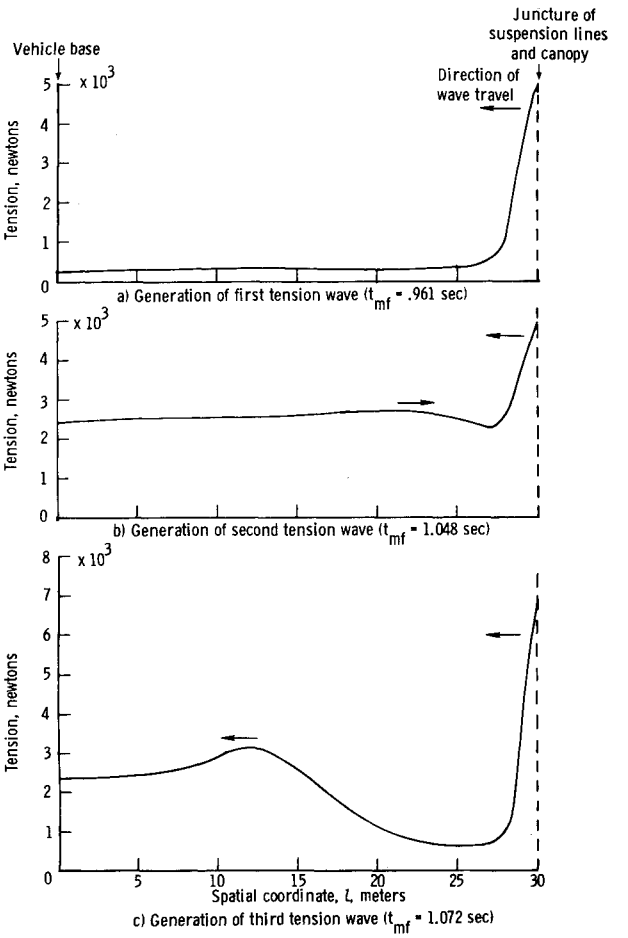

Fig. 5 Computed profiles of tension in suspension lines during BLDT AV-4 parachute deployment.

corresponding to mortar fire, line stretch and estimated bag strip.

A sequence of tension profiles computed during simulation of the canopy unfurling phase of the AV-4 flight test are shown in Fig. 5. Figure 5a shows the first tension wave, which is generated by the unfurling of the mass concentration at the leading edge of the band portion of the canopy, as it leaves the juncture of the suspension lines and canopy. Figure 5b shows a second tension wave, which is generated by the unfurling of the mass concentration at the trailing edge of the band, leaving the juncture as the damped first wave is propagating back toward the juncture after having been reflected at the vehicle boundary. Figure 5c shows a third tension wave, which is generated by the unfurling of the leading edge of the disk section of the canopy, leaving the juncture as the damped second wave approaches the vehicle. Similar tension profiles were computed during simulation of the canopy unfurling phase of the B/L-2 flight test.

Histories of the computed tension at the vehicle attachment point are compared with flight-test data histories in Fig. 6, for B/L-2, and in Fig. 7, for AV-4. Peak loads shown in the initial half of each flight-test data history are attributed to phenomena which are not associated with the dynamics of unfurling, and, as such, are not included in the present mathematical model. Agreement of occurrence times of peak loads between the computed and flight-test data histories is very good. Although agreement in peak load magnitudes is only fair, the results computed using the present method show considerable improvement over the results obtained using the massless-spring model of Ref. 3. Lack of agreement in peak load magnitudes is an inherent result of the idealizations present in the development of the present model. The most significant of these is probably

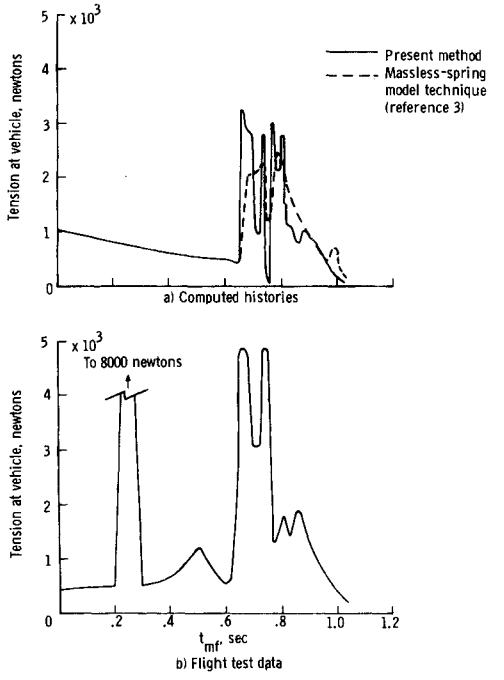

Fig. 6 Comparison of computed and flight-test histories of tension at vehicle during PEPP B/L-2 parachute deployment.

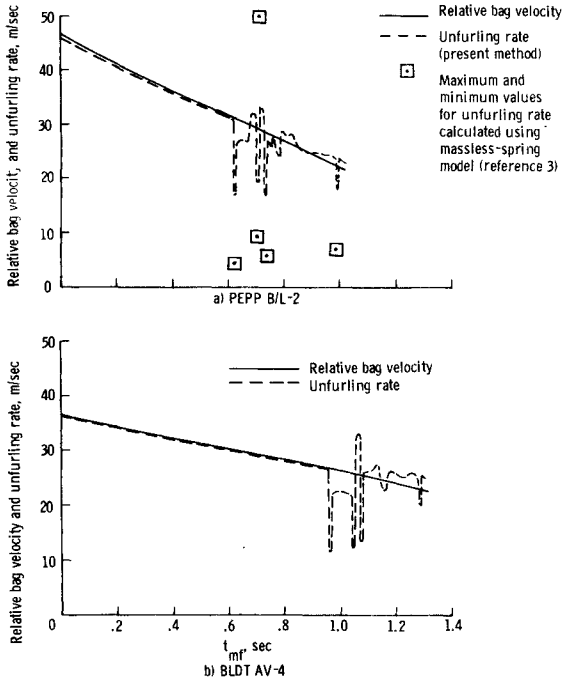

Fig. 8 Computed histories of relative bag velocity and unfurling rate for PEPP B/L-2 and BLDT AV-4.

the assumption of no deflection at the vehicle boundary; for an actual flight configuration the conditions at the boundary are unknown.

Computed histories of relative deployment bag velocity and unfurling rate for the two flight tests are presented in Fig. 8. The general trend of both the relative bag velocity and the unfurling rate is a smooth decay due to deceleration of the towing vehicle. However, sharp decreases in the unfurling rate occur when sudden increases in the linear mass density of the unfurling parachute are encountered; conversely, when sudden decreases in the linear mass density are encountered, the unfurling rate increases sharply. It is evident in the histories presented for the B/L-2 flight, that fluctuations in the unfurling rate computed using the presented method are much less severe than those fluctuations computed using the massless-spring technique of Ref. 3. Although there is an absence of data concerning unfurling rate, the magnitudes computed using the present method are thought to be good approximations to the magnitudes experienced during the flight tests being studied.

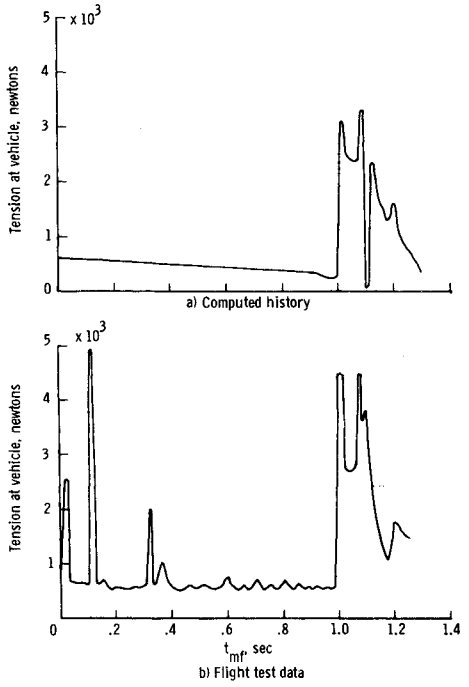

Fig. 7 Comparison of computed and flight-test histories of tension at vehicle during BLDT AV-4 parachute deployment.

Conclusions

A new mathematical model has been presented for calculating planar motions and loads of the lines-first parachute unfurling process. The unfurling process has been treated as two distinct phases: a suspension-line unfurling phase, during which a massless-spring model of the suspension-line elasticity is employed; and a canopy unfurling phase, during which an idealized continuum model of the suspension lines is employed. Based on comparisons of the results obtained using the present model with experimental data from two disk-gap-band parachute flight tests the following conclusions can be made:

1) Computed histories of unfurled length agree very well with flight-test data.

2) Computed histories of tension at the vehicle agree well, in general, with flight-test data histories, with remaining inaccuracies being attributed to the idealizations included in the mathematical model.

3) Fluctuations in computed histories of unfurling rate are much less severe than those calculated using a massless-spring-type model of suspension-line elasticity. The histories computed using the present model are thought to be good approximations to the unfurling rates experienced during the flight-tests being studied.

References

[1] Whitlock, C. H., "Advances in Modeling Aerodynamic Decelerator Dynamics," *Astronautics and Aeronautics*, Vol. 11, No. 4, April 1973, pp. 67–71.

[2] Huckins, E. K., III, "Techniques for Selection and Analysis of Parachute Deployment Systems," TN D-5619, 1970, NASA.

[3] Poole, L. R. and Huckins, E. K., III, "Evaluation of Massless-

Spring Modeling of Suspension-Line Elasticity During the Parachute Unfurling Process," TN D-6671, 1972, NASA.

[4] Huckins, E. K., III, "A New Technique for Predicting the Snatch Force Generated During Lines-First Deployment of an Aerodynamic Decelerator," *Journal of Spacecraft and Rockets*, Vol. 8, No. 3, March 1971, pp. 298–299.

[5] Poole, L. R., "Numerical Solution of Equations Governing Longitudinal Suspension-Line Wave Motion During the Parachute Unfurling Process," M.S. thesis, May 1973, George Washington Univ., Washington, D.C.

[6] Bendura, R. J., Huckins, E. K., III, and Coltrane, L. C., "Performance of a 19.7-Meter-Diameter Disk-Gap-Band Parachute in a Simulated Martian Environment," TM X-1499, 1968, NASA.

[7] Dickinson, D., Schlemmer, J., Hicks, F., Michel, F., and Moog, R. D., "Balloon-Launched Decelerator Test Program Post-Flight Test Report, BLDT Vehicle AV-4," CR-112179, 1972, NASA.

JANUARY 1974 AIAA JOURNAL VOL. 12, NO. 1

Unsteady Aerodynamic Response of a Two-Dimensional Airfoil at High Reduced Frequency

G. L. COMMERFORD* AND F. O. CARTA†
United Aircraft Research Laboratories, East Hartford, Conn.

An experimental technique is described which corroborates the predictions of several new analyses of the unsteady response of an airfoil to high frequency flow fluctuations. The periodically fluctuating flowfield was produced by the natural shedding of vortices from a transverse cylinder to yield a reduced frequency of 3.9 based on airfoil semichord. Unsteady pressure measurements were made on an instrumented airfoil mounted downstream and above the turbulent wake of the cylinder. These unsteady pressures were found to be in good agreement with current compressible theories and show a chordwise variation of pressure phase angle which is not predicted by the incompressible analysis of Sears. Large reductions of the unsteady lift and phase angle were also observed for large airfoil incidence angles.

Nomenclature

a	= speed of sound
b	= airfoil semichord
C_L, C_M	= lift and moment coefficients
$C(k)$, $S(k)$, $T(k)$	= unsteady aerodynamic functions
f	= frequency
k	= reduced frequency, $b\omega/U$
M	= Mach number, U/a
q	= dynamic pressure, $\rho U^2/2$
$S^*(k)$	= modified unsteady lift function
u, v	= horizontal and vertical velocity perturbations
U	= freestream velocity
y	= vertical coordinate
α	= angle of attack
Γ	= vortex strength
ΔL	= incremental lift
Δp	= differential pressure
λ	= wavelength
ρ	= density
ϕ	= phase angle
ω	= frequency

Subscripts

o	= amplitude
v	= vertical
H	= horizontal
R	= real
I	= imaginary
S	= quasi-steady

Superscripts

*	= nondimensional coordinate
¯	= time-independent amplitude

Presented as Paper 73-309 at the AIAA Dynamics Specialists Conference, Williamsburg, Va., March 19–20, 1973; received April 25, 1973; revision received August 24, 1973. This work was done in support of the Pratt & Whitney Aircraft Division of United Aircraft Corporation under NASA Contract NASW-1908, "Aerodynamic Broadband Noise Mechanisms Applicable to Axial Compressors."

Index categories: Nonsteady Aerodynamics; Aeroelasticity and Hydroelasticity.

* Formerly Research Engineer, Aeroelastics Group; presently Member of Technical Staff, Space Division, Rockwell International. Member AIAA.

† Supervisor, Aeroelastics Group. Associate Fellow AIAA.

Introduction

IN computing the time-dependent forces and moments acting on an aerodynamic body, both the aeroelastician and the acoustician must necessarily consider an unsteady flowfield. This is because the physical processes in both cases involve relative motions at high frequency between the aerodynamic body and the airstream. Thus, an unsteady wake is produced which has an influence on the aerodynamic body and which is dependent on both time and distance. In general, the most important direct effects of unsteadiness are 1) phase differences between the aerodynamic forces and the motion producing them, and 2) an attenuation of the lift vector.

The unsteady aerodynamic theory associated with the flutter problem was derived in 1935 by Theodorsen.[1] He found that the unsteady lift or moment on an airfoil oscillating in both pitching and plunging could be expressed as functions of the respective quasi-steady lift (lift neglecting the influence of wake vortices on the flow) or moment, and a complex function, $C(k)$, known appropriately as the Theodorsen function. Sears[2] solved the similar problem of a stationary airfoil passing through a sinusoidally varying transverse gust. He found that the unsteady lift was equal to the steady lift at the effective gust angle of attack multiplied by a complex function $S(k)$, known as the Sears function.

The functions $C(k)$ and $S(k)$ are not significantly different at low reduced frequencies ($k < 0.3$) (cf. Refs. 3 and 4). However, as the reduced frequency becomes large ($k > 0.6$) the differences